

RESEARCH

Open Access



Loss of glucosylceramide synthase impairs the growth and virulence of *Fusarium oxysporum* f. sp. *cubense*

Jian Wang^{1,3}, Kun Zhang^{1,2}, Li-Qun Huang^{1,2}, He-Nan Bao^{1,2}, Na Hai^{1,2}, Yu-Bing Yang^{1,2}, Si-Wen Liu⁴, Chun-Yu Li⁴ and Nan Yao^{1,2,3*} 

Abstract

Glucosylceramides are a class of membrane lipids that serve as vital structural and signaling molecules in eukaryotes. In this study, we explored the function of *FocGCS*, a glucosylceramide synthase (GCS) in *Fusarium oxysporum* f. sp. *cubense* tropical race 4 (*Foc* TR4) that causes Fusarium wilt in banana plants. *FocGCS* is highly expressed in germinating conidia and during early infection stage of *Foc* TR4. Disruption of *FocGCS* resulted in severely retarded vegetative growth, reduced conidiation, and production of morphologically abnormal conidia. Sphingolipid profiling revealed that the *FocGCS* null mutant lacks glucosylceramide. Pathogenicity assays on banana plants revealed substantial loss of virulence in the *FocGCS* null mutant. Moreover, biochemical analyses indicated that *FocGCS* is involved in cell wall integrity but is not required for oxidative and osmotic stress tolerance in *Foc* TR4. Transcriptome analysis suggested that disruption of *FocGCS* strongly affects transmembrane transport in *Foc* TR4. Our findings show that GCS is essential for normal fungal growth and pathogenesis in *Foc* TR4.

Keywords: *Fusarium oxysporum* f. sp. *cubense* tropical race 4, Glucosylceramide, Sphingolipid, Virulence, Conidiation, Cell wall integrity

Background

The soil-borne anamorphic fungus *Fusarium oxysporum* f. sp. *cubense* (*Foc*) colonizes and blocks the vascular system of host plants, causing Fusarium wilt (also known as Panama disease), the most destructive fungal disease on banana plants worldwide (Ploetz 2006; Fourie et al. 2009). In general, *Foc*-infected banana plants die before they produce bunches of fruit, and this has led to reduced banana yields in Asia, Africa, Australia, and the tropical Americas in the past few decades (Li et al. 2011; Liu et al. 2019a). Based on its host types, *Foc* can be classified

into four races (Ploetz 2006; Dita et al. 2010). *Foc* tropical race 4 (*Foc* TR4) is highly pathogenic to almost all banana cultivars and has destroyed thousands of hectares of Cavendish bananas in tropical and subtropical countries (Molina et al. 2009; Zuo et al. 2015). To date, there are no effective biological, chemical, and cultural measures to manage this disease (Ploetz 2015).

Glucosylceramides (GlcCers) are common membrane sphingolipids in most eukaryotic organisms. Glucosylceramide synthase (GCS) catalyzes the transfer of a sugar residue from UDP-glucose to ceramide to form GlcCer (Wang et al. 2021). Although the *GCS* gene is absent in *Saccharomyces cerevisiae*, it is present in most of the other fungal species studied so far, such as phytopathogens *Magnaporthe grisea*, *Colletotrichum gloeosporioides*, and *Fusarium graminearum* (Leipelt et al. 2001; Dickson and Lester 2002; Ramamoorthy et al.

*Correspondence: yaonan@mail.sysu.edu.cn

¹ State Key Laboratory of Biocontrol and Guangdong Provincial Key Laboratory of Plant Resource, Sun Yat-sen University, Guangzhou 510275, China

Full list of author information is available at the end of the article



© The Author(s) 2022. **Open Access** This article is licensed under a Creative Commons Attribution 4.0 International License, which permits use, sharing, adaptation, distribution and reproduction in any medium or format, as long as you give appropriate credit to the original author(s) and the source, provide a link to the Creative Commons licence, and indicate if changes were made. The images or other third party material in this article are included in the article's Creative Commons licence, unless indicated otherwise in a credit line to the material. If material is not included in the article's Creative Commons licence and your intended use is not permitted by statutory regulation or exceeds the permitted use, you will need to obtain permission directly from the copyright holder. To view a copy of this licence, visit <http://creativecommons.org/licenses/by/4.0/>.

2007; Del Poeta et al. 2014; Huang et al. 2019). Several studies have suggested that GlcCer modulates membrane physical properties and physiological functions in some fungal pathogens of humans to facilitate fungal growth, spore germination, virulence, and hyphal development and differentiation (Levery et al. 2002; Warnecke and Heinz 2003; Thevissen et al. 2004; Ramamoorthy et al. 2007; Zhu et al. 2014). In the human fungal pathogen *Cryptococcus neoformans*, GlcCer is essential for fungal growth and is a key virulence factor (Rittershaus et al. 2006). The GlcCer of *C. neoformans* is a fungal antigen that plays a role in cell wall synthesis and yeast budding. The antibodies against *C. neoformans* GlcCer produced by patients with cryptococcosis inhibit hyphal growth and cell division *in vitro* (Rodrigues et al. 2000). In *Candida albicans*, GlcCer biosynthesis is an important determinant of virulence in a murine model (Noble et al. 2010). In *Aspergillus nidulans* and *Aspergillus fumigatus*, inhibiting GlcCer synthesis using 1-phenyl-2-decanoylamino-3-morpholino-1-propanol (PDMP), an inhibitor of GCS in mammalian cells, adversely affected fungal growth and spore germination (Levery et al. 2002). In the phytopathogen *Penicillium digitatum*, deletion of *PdGcs1* resulted in impaired virulence on citrus fruits (Zhu et al. 2014). In *C. gloeosporioides*, *CgGCS*-knockout mutants almost completely lost the ability to invade natural host plants tomato (*Solanum lycopersicum*) and mango (*Mangifera indica*) (Huang et al. 2019). However, the role of GCS in pathogenesis of *F. graminearum* is host-dependent (Ramamoorthy et al. 2007). The results of these studies indicate that GlcCers are involved in the growth and virulence of various fungal pathogens.

Additionally, antifungal defensins, which are cationic antimicrobial proteins and part of plant innate immunity, bind to distinct GlcCers in the membranes of fungi and inhibit fungal growth. For instance, the defensin RsAFP2 produced by *Raphanus sativus* interacts specifically with GlcCers from *Pichia pastoris* and *C. albicans*, resulting in growth arrest of the pathogens (Thevissen et al. 2004). The defensin MsDef1 from *Medicago* spp. interacts with GlcCer produced by *F. graminearum*, inhibiting fungal growth (Ramamoorthy et al. 2007). Together, these studies suggest that fungal GlcCer and GCS are promising biologically active targets for new antimicrobials (Nimrichter and Rodrigues 2011).

In this study, we report the identification and functional analysis of GCS in *Foc* TR4. We found that *FocGCS* is a key regulator of fungal growth and conidiation and is indispensable for cell wall integrity and full virulence of *Foc* TR4.

Results

Characterization of *FocGCS*

Using BLASTp, we found a putative GCS-encoding gene (XP_031069237.1) in *Foc* TR4, which is homologous to the GCS genes in *Homo sapiens* (NP_003349.1), *C. albicans* (KGU07664.1), and *F. graminearum* (XP_011324566.1), with 23.73%, 34.41%, and 68.05% amino acid identity, respectively (Additional file 1: Table S1). Analysis of the amplified 1815-bp genomic and 1578-bp cDNA sequences indicated that *FocGCS* contains a single 51-bp intron, and the entire coding sequence of the gene is 1581 bp, encoding a protein of 526 amino acids with an estimated molecular mass of 58.8 kDa.

The predicted *FocGCS* protein contains a conserved Glyco_tranf_21 domain, an N-terminal transmembrane domain, and three C-terminal transmembrane domains (Additional file 2: Figure S1a). These domains, including the D1, D2, D3, and Q/RXXXRW motifs (Additional file 2: Figure S1b), are essential for the enzymatic activity of mammalian GCS; histidine 193 is conserved in the Glyco_tranf_21 domain (Leipelt et al. 2001). Phylogenetic analysis indicated that *FocGCS* is closely related to GCSs from *F. graminearum*, *Pyricularia oryzae*, *Beauveria bassiana*, *C. gloeosporioides*, and *Verticillium dahliae*, with 68.05%, 47.32%, 50.75%, 53.83%, and 50.64% amino acid sequence identity, respectively (Fig. 1a), indicating that *FocGCS* is well conserved in fungi. Based on amino acid sequence similarity of GCSs, the most distantly related fungus of *Foc* TR4 in the phylogenetic tree is *Rhizoctonia solani* (30.95% identity). *FocGCS* has 23.73% and 11.14% amino acid sequence identity to GCSs from *Homo sapiens* and *Arabidopsis thaliana*, respectively.

FocGCS is highly expressed at different developmental stages and during early infection stage of *Foc* TR4

To examine the expression of *FocGCS* at different developmental stages of *Foc* TR4, we constructed the *FocGCS*-GFP fusion cassette, which expresses *FocGCS* fused to green fluorescent protein (GFP) under the control of the *FocGCS* promoter. When expressed in the $\Delta FocGCS$ -C-GFP strain described below, the *FocGCS*-GFP protein was observed in conidia and hyphae, especially in the Golgi, endoplasmic reticulum, and vacuole, whereas fluorescent signals produced by the *Foc*-GFP strain, which expresses an un-fused GFP, was observed throughout conidia and hyphae (Additional file 2: Figure S2).

We investigated the transcript level of *FocGCS* in mycelia, conidia, germinating conidia, and *Foc* TR4-infected banana roots at different time points of early infection by quantitative real-time PCR (qPCR). Compared with that in mycelia, *FocGCS* transcript level showed a several-fold increase during conidial germination (Fig. 1b).

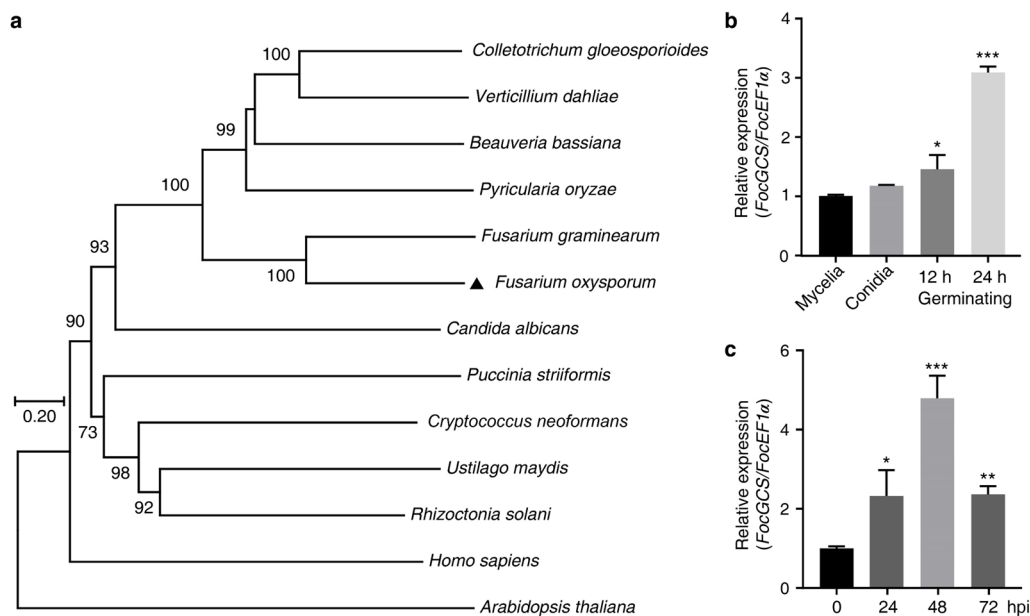


Fig. 1 The expression and phylogenetic analysis of *FocGCS*. **a** Phylogenetic tree of putative GCS proteins identified in different organisms. Values on the branches of clusters represent the results of bootstrap analysis (10,000 bootstrap replicates). *Verticillium dahliae* (XP_009653962.1); *Colletotrichum gloeosporioides* (EQB52767.1); *Beauveria bassiana* (KAF1734959.1); *Pyricularia oryzae* (XP_003710106.1); *Fusarium graminearum* (XP_011324566.1); *Fusarium oxysporum* f. sp. *cubense* tropical race 4 (black triangle, XP_031069237.1); *Candida albicans* (KGU07664.1); *Puccinia striiformis* (KNF02135.1); *Cryptococcus neoformans* (AAX55972.1); *Ustilago maydis* (XP_011390830.1); *Rhizoctonia solani* (CUA72326.1); *Homo sapiens* (NP_003349.1); *Arabidopsis thaliana* (At2g19880). **b** Transcript levels of *FocGCS* at different fungal developmental stages. Asterisks indicate significant difference from the mycelia group (Student's t-test, * $P < 0.05$, *** $P < 0.001$). **c** Transcript levels of *FocGCS* in infected banana roots. The *FocEF1a* gene was used as an internal control to normalize the data for comparing the relative transcript abundance. Asterisks indicate significant differences from the control group (Student's t-test, * $P < 0.05$, ** $P < 0.01$, and *** $P < 0.001$). The mean values \pm SD were calculated from three independent experiments

In addition, in *Foc* TR4-inoculated plants, the transcript level of *FocGCS* increased gradually during the early infection stages until 48 h post-infection (hpi) and then decreased (Fig. 1b, c).

Generation of *FocGCS*-knockout mutant and complemented strain

To explore the role of *FocGCS*, we generated *FocGCS*-knockout mutant using a targeted gene replacement strategy. Hygromycin B 4-O-kinase-coding gene (*HPH*) driven by the *TrpC* promoter was transformed into the *Foc* TR4 strain II5 via homologous recombination to replace the *GCS* gene (Additional file 2: Figure S3a). The putative mutants were screened by PCR with the primer pairs listed in Additional file 1: Table S2. PCR amplification of the 5' and 3' terminus of *FocGCS* with the primer pairs 1/2 and 3/4 produced a 1983-bp and a 1951-bp fragment, respectively, in the $\Delta FocGCS$ mutant, but not in the wild-type (WT) strain, suggesting correct integration of *HPH* (Additional file 2: Figure S3b). qPCR analysis detected no *GCS* transcript in the $\Delta FocGCS$ mutant (Additional file 2: Figure S3c). Southern blotting of genomic DNA using a 502-bp *FocGCS*-specific probe

revealed the presence of a 7.5-kb *Xba*I fragment in the WT strain, but not in the $\Delta FocGCS$ mutants (Fig. 2a), demonstrating targeted disruption of the *FocGCS* gene in the mutants.

Complementation of the $\Delta FocGCS$ mutant was performed with the *FocGCS*-GFP construct described above. This construct was introduced into a representative $\Delta FocGCS$ strain to produce the complemented $\Delta FocGCS$ -C-GFP strain. Several neomycin-resistant transformants were selected and verified by PCR amplification, which produced a 980-bp fragment identical to that obtained from the WT strain but absent from the $\Delta FocGCS$ mutant (Additional file 2: Figure S3b). qPCR analysis revealed that the *GCS* transcript level in the complemented strain was similar to that in the WT strain (Additional file 2: Figure S3c).

FocGCS plays important roles in vegetative growth and conidiation of *Foc* TR4

To determine whether *FocGCS* is involved in vegetative growth of *Foc* TR4, we assessed the growth phenotype of $\Delta FocGCS$, $\Delta FocGCS$ -C-GFP, and WT strains. The $\Delta FocGCS$ mutant grew 38% slower than the WT and

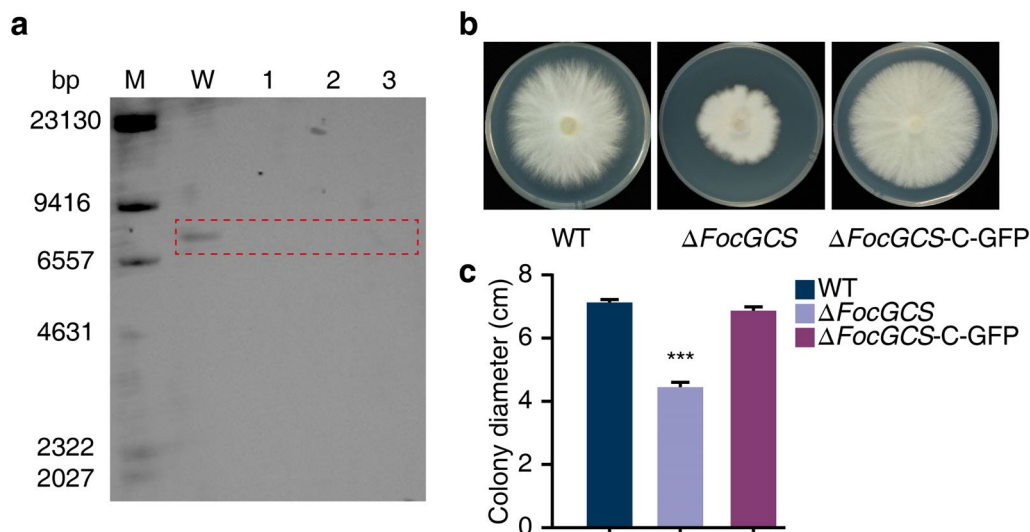


Fig. 2 Southern blot identification and growth phenotype of the $\Delta FocGCS$ mutant. **a** Southern blot analysis of genomic DNA extracted from the WT and three putative $\Delta FocGCS$ strains and digested with *Xba*I. **b** Colony morphology of the WT, $\Delta FocGCS$, and $\Delta FocGCS$ -C-GFP strains on PDA plates. Photos were taken after incubation at 28 °C for 5 days. **c** Colony diameters of the WT, $\Delta FocGCS$, and $\Delta FocGCS$ -C-GFP strains grown on PDA plates. The mean values \pm SD were calculated from three independent experiments, and asterisks indicate significant differences from the WT group (Student's *t*-test, ****P* < 0.001)

$\Delta FocGCS$ -C-GFP strains on potato dextrose agar (PDA) (Fig. 2b, c). Further microscopic observation revealed that $\Delta FocGCS$ produced fewer macroconidia than the WT and $\Delta FocGCS$ -C-GFP strains (Fig. 3a). The macroconidia of the mutant strain had only a single septum and displayed morphological defects, with a 57% reduction in length compared with the WT and complemented strains (Fig. 3a, b). In addition, the mutant strain produced significantly fewer conidia (94% reduction) than the WT and complemented strains (Fig. 3c), and the germination rate of conidia of the mutant was much lower than those of the WT and complemented strains (Fig. 3d). These results indicate that targeted disruption of *FocGCS* resulted in retarded vegetative growth, reduced conidial production and germination, and abnormal conidial morphology in *Foc TR4*.

FocGCS* is required for GlcCer biosynthesis in *Foc TR4

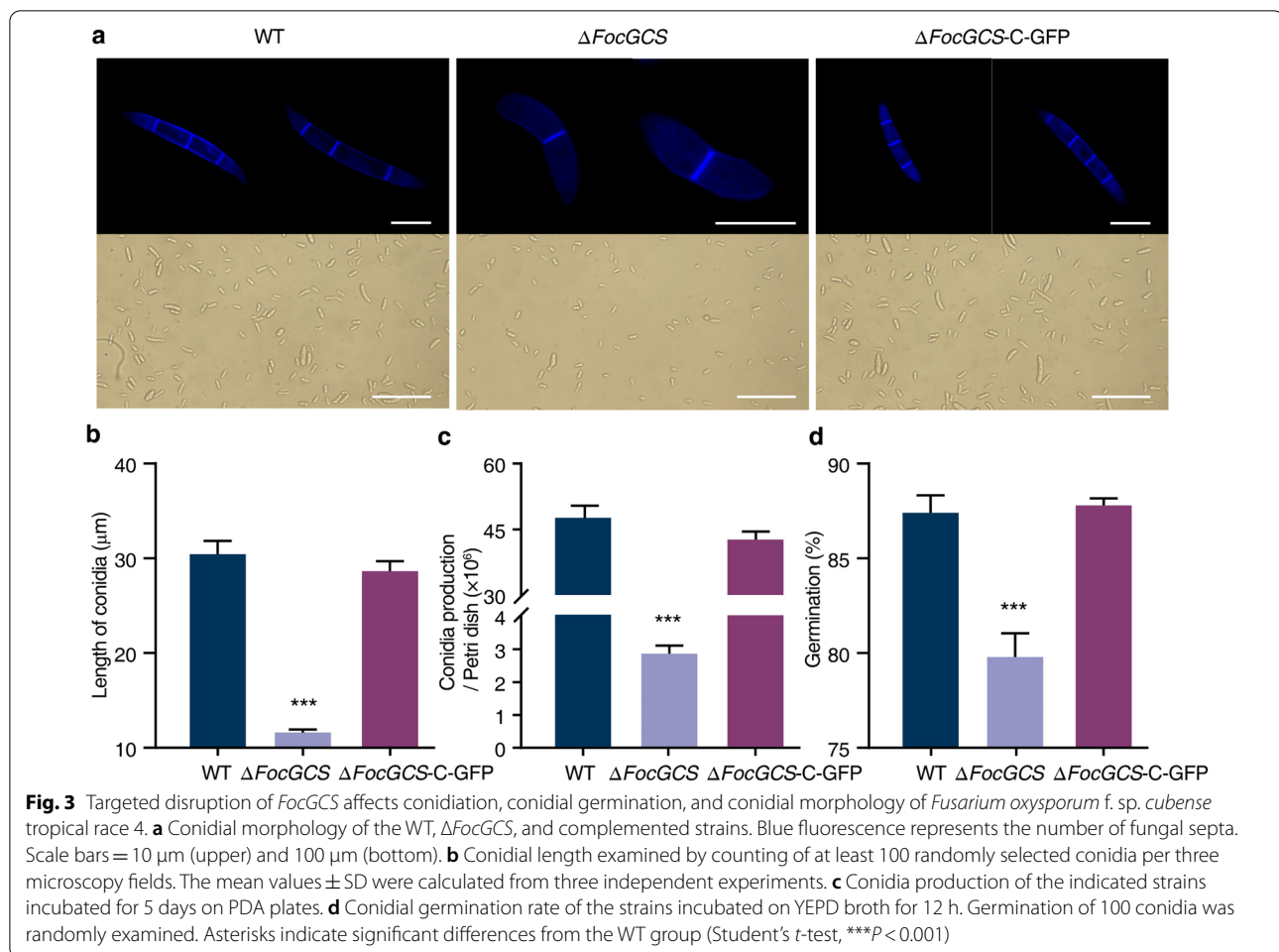
To examine whether targeted disruption of *FocGCS* affects the biosynthesis of sphingolipids, we compared the contents of GlcCers, hydroxyceramides (hCers), ceramides (Cers), and long chain bases (LCBs) in hyphae of the WT and mutant strains using high-performance liquid chromatography-mass spectrometry/mass spectrometry (HPLC-MS/MS). The GlcCers d19:2 g18:0, d19:2 g18:1, d19:2 g20:0, and d19:2 g24:0 were almost undetectable in the $\Delta FocGCS$ mutant (Fig. 4a, d). By contrast, the amounts of hCers d19:2 h18:0, d19:2 h18:1, d19:2 h20:0, and d19:2 h24:0 were significantly higher in the mutant

strain than those in the WT strain (Fig. 4b and Additional file 2: Figure S4). As shown in Fig. 4c, the total amount of hCers was approximately sixfold greater in the mutant strain than that in the WT strain, while the total amount of GlcCers was much lower in the mutant strain than that in the WT strain. There was no significant difference in accumulation levels of LCBs and Cers between the WT and mutant strains. These results indicate that targeted disruption of *FocGCS* resulted in increased accumulation of hCers whereas reduced accumulation of GlcCers, suggesting that *FocGCS* functions as a glucosylceramide synthase in *Foc TR4*.

FocGCS* contributes to the full virulence of *Foc TR4

To determine whether disruption of *FocGCS* affects the virulence of *Foc TR4*, pathogenicity test was conducted on Cavendish banana plantlets at the 6–7 leaf stage through root infection assays. The WT- and $\Delta FocGCS$ -C-GFP-inoculated plants showed severe disease symptoms at 4 weeks post-inoculation. In comparison, the degree of browning in inner rhizome of $\Delta FocGCS$ -inoculated plants was significantly reduced (Fig. 5a). Disease severity in $\Delta FocGCS$ -inoculated plants was dramatically lower than that in plants inoculated with other tested strains (Fig. 5b).

To determine whether *FocGCS* knockout affects fungal growth *in planta*, we quantified fungal biomass of the WT, $\Delta FocGCS$, and $\Delta FocGCS$ -C-GFP strains in root tissues. The fungal biomass in banana roots inoculated with



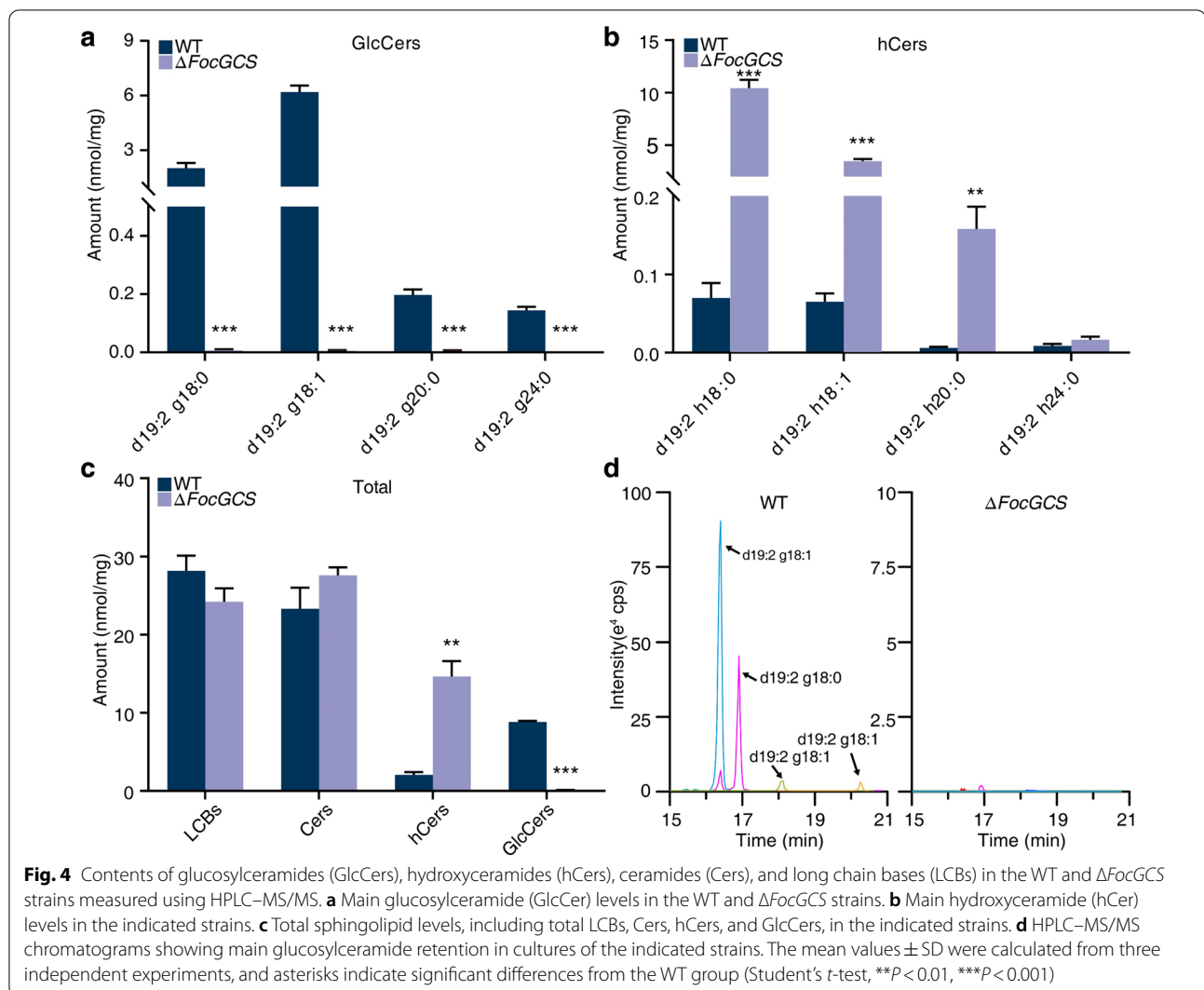
$\Delta FocGCS$ was significantly reduced compared with that in WT-inoculated roots at 5, 10, and 15 days post-inoculation (dpi) (Fig. 5c). These data suggest that knockout of *FocGCS* retarded mycelial extension rate of *Foc* TR4 within banana roots and reduced the virulence of the pathogen on banana plants.

FocGCS affects cell wall integrity of *Foc* TR4

GlcCers are essential structural components of fungal cell wall, plasma membrane, and intracellular vesicles (Ramamoorthy et al. 2007; Fernandes et al. 2016). Therefore, we analyzed the sensitivity of the WT, $\Delta FocGCS$, and $\Delta FocGCS$ -C-GFP strains to cell-wall-damaging agents (0.2% Calcofluor white (CFW) or 0.2% Congo red (CR)). After 5 days of incubation on PDA plates supplemented with or without the agent, the mutant strain showed increased CFW and CR resistance compared with the WT and complemented strains (Fig. 6a). The growth inhibition rate of the $\Delta FocGCS$ mutant decreased by 25% and 19% on CFW and CR plates, respectively, compared

with that of the WT strain (Fig. 6b), indicating that the mutant was more resistant to cell-wall-perturbing agents.

Considering that chitin is also the major component of fungal cell wall, and CFW and CR inhibit fungal cell wall assembly by binding to chitin, the chitin contents in the WT, $\Delta FocGCS$, and $\Delta FocGCS$ -C-GFP strains were also compared (Schoffelmeer et al. 1999). The results showed that the chitin content in the mutant was 33% and 27% higher than that in the WT and complemented strains, respectively (Fig. 6c). Apparent changes in cell wall structure were observed in $\Delta FocGCS$ strains under transmission electron microscopy (TEM), including thickening of the cell wall and formation of more fungal-type vacuole (Fig. 6d), and the thickness of the cell wall in $\Delta FocGCS$ strain increased by 22% compared with that of the WT strain (Fig. 6e). These results indicate that *FocGCS* is involved in cell wall integrity and chitin biosynthesis of *Foc* TR4.



***FocGCS* is not involved in the tolerance of *Foc TR4* to oxidative and osmotic stresses**

The production of reactive oxygen species is necessary for full virulence of *Foc TR4* and plant defense (Qi et al. 2013). We therefore investigated whether *FocGCS* is involved in oxidative stress response by exposing the WT, $\Delta FocGCS$, and $\Delta FocGCS$ -C-GFP strains to 0.5 mM H_2O_2 (Fig. 7a). The difference in mycelial growth rate between these three strains was not significant (nearly 65% inhibition for all the strains), indicating that *FocGCS* is not essential for tolerance to oxidative stress in *Foc TR4* (Fig. 7a, b).

Because GlcCer mainly functions as structural component of cell membrane, we speculated that GlcCer defect might influence the response to osmotic stress. We therefore examined the growth of the WT, $\Delta FocGCS$, and $\Delta FocGCS$ -C-GFP strains on PDA plates supplemented with NaCl or sorbitol. No differences in colony growth

were observed among the three strains incubated on the plates containing 1 M NaCl or 1 M sorbitol (Fig. 7a, c). These findings indicate that *FocGCS* is not necessary for osmoregulation in *Foc TR4*.

GlcCers have been reported to be involved in regulating pH tolerance (Rittershaus et al. 2006; Ramamoorthy et al. 2007). However, the WT, $\Delta FocGCS$, and $\Delta FocGCS$ -C-GFP strains exhibited similar pH-dependent growth trends, with the $\Delta FocGCS$ mutant showing greater inhibition at pH 10 (Fig. 7d, e). These results suggest that GlcCer in *Foc TR4* does not broadly participate in environmental pH regulation but may influence alkali tolerance.

Comparative transcriptome analysis between the *Foc TR4* WT strain and the $\Delta FocGCS$ mutant

To comprehensively investigate the difference in gene expression between the $\Delta FocGCS$ mutant and the WT

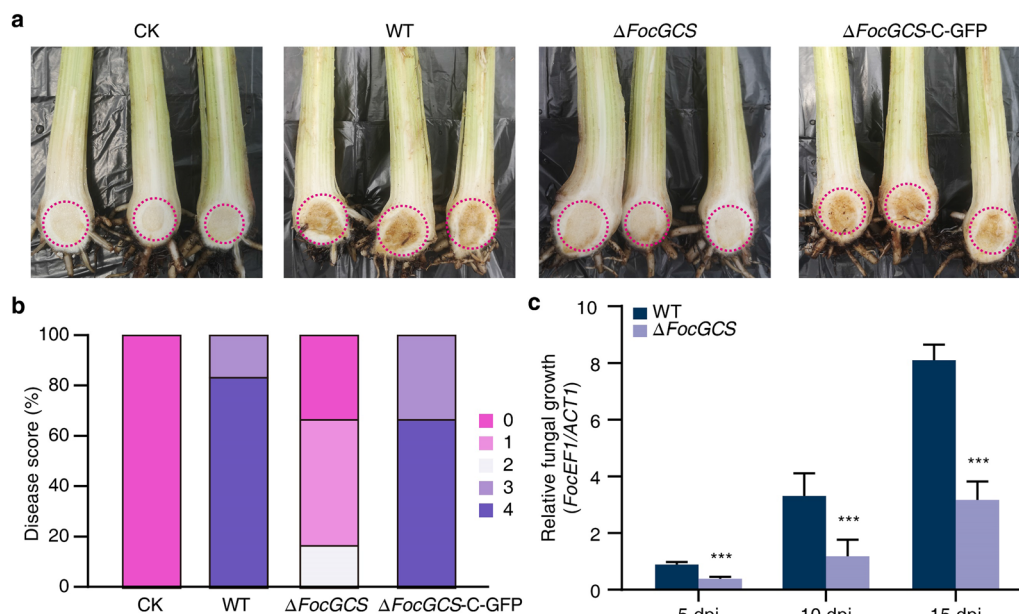


Fig. 5 *FocGCS* is required for full virulence of *Fusarium oxysporum* f. sp. *cubense* tropical race 4. **a** Symptoms on banana roots at 30 days post-inoculation (dpi). The Cavendish banana variety Brazilian (*Musa* spp. AAA group) was inoculated with the WT, $\Delta FocGCS$, and complemented strains. Images are representative of three independent experiments. **b** Disease score of the inoculated banana plants at 30 dpi. Disease severity was assessed on a scale of 0–4. The disease score (%) = (the number of inoculated banana plants with different disease severity) / (the number of total inoculated banana plants) \times 100. **c** Fungal biomass in roots of the inoculated plants. Relative fungal growth *in planta* was evaluated by qPCR analysis of *FocEF1a* and banana *ACT1* and shown as a ratio of *FocEF1a/ACT1*. The mean values \pm SD were calculated from three independent experiments, and asterisks indicate significant differences from the WT group (Student's *t*-test, ****P* < 0.001)

strain, we performed comparative transcriptome analysis. The results showed that 571 genes exhibited at least a twofold difference in expression between the WT and mutant strains (Additional file 3: Table S3). Functional classification of differentially expressed genes (DEGs) was further conducted to explore the transcriptome regulation pattern. DEGs matching well-characterized proteins or proteins with putative functions were grouped according to their Gene Ontology (GO) categories, as summarized in Additional file 3: Table S3. Most DEGs identified in this study were assigned to different biological and molecular function categories. These DEGs encode proteins that are predicted to be involved in the oxidation and reduction, ion binding, and transmembrane processes (Fig. 8a, b). ‘Transmembrane transport’ and ‘Transmembrane transporter activity’ were the most significantly enriched GO terms for these DEGs (Fig. 8c), implying that interrupting transmembrane transport in the mutant strain may account, in part, for the differences between the $\Delta FocGCS$ mutant and the *Foc* TR4 WT strain.

Discussion

GlcCers are important membrane lipids in animals, plants, and fungi. In this study, we identified a *GCS* gene, termed *FocGCS*, in *Foc* TR4, with the goal to determine

its role in fungal growth, development, and virulence. *FocGCS* shares substantial sequence identity with homologs in other fungi (Additional file 2: Figure S1b and Additional file 1: Table S1) (Leipelt et al. 2001). Our findings demonstrate that *FocGCS* encodes a *bona fide* GCS whose product, GlcCer, is essential for regulating fungal growth, conidiation, conidial germination, cell wall integrity, and virulence of *Foc* TR4.

Unlike in *S. cerevisiae*, GlcCers are produced in filamentous and dimorphic fungi, such as *C. albicans*, *F. graminearum*, and *P. digitatum* (Dickson and Lester 2002; Ramamoorthy et al. 2007; Noble et al. 2010; Zhu et al. 2014). Disruption of *GCS* can reduce mycelial growth and virulence of pathogenic fungi (Rittershaus et al. 2006; Ramamoorthy et al. 2007; Zhu et al. 2014; Huang et al. 2019). In our study, deletion of *FocGCS* severely retarded the growth of *Foc* TR4 (38% reduction in growth rate compared with the WT and complemented strains) (Fig. 2b, c), indicating that *GCS* is essential for normal growth of the pathogen. We speculate that growth deficiency in *Foc* TR4 may contribute to its impaired pathogenesis. Furthermore, knockout of *FocGCS* reduced the virulence of *Foc* TR4 on host plants, consistent with the previous studies (Zhu et al. 2014; Huang et al. 2019).

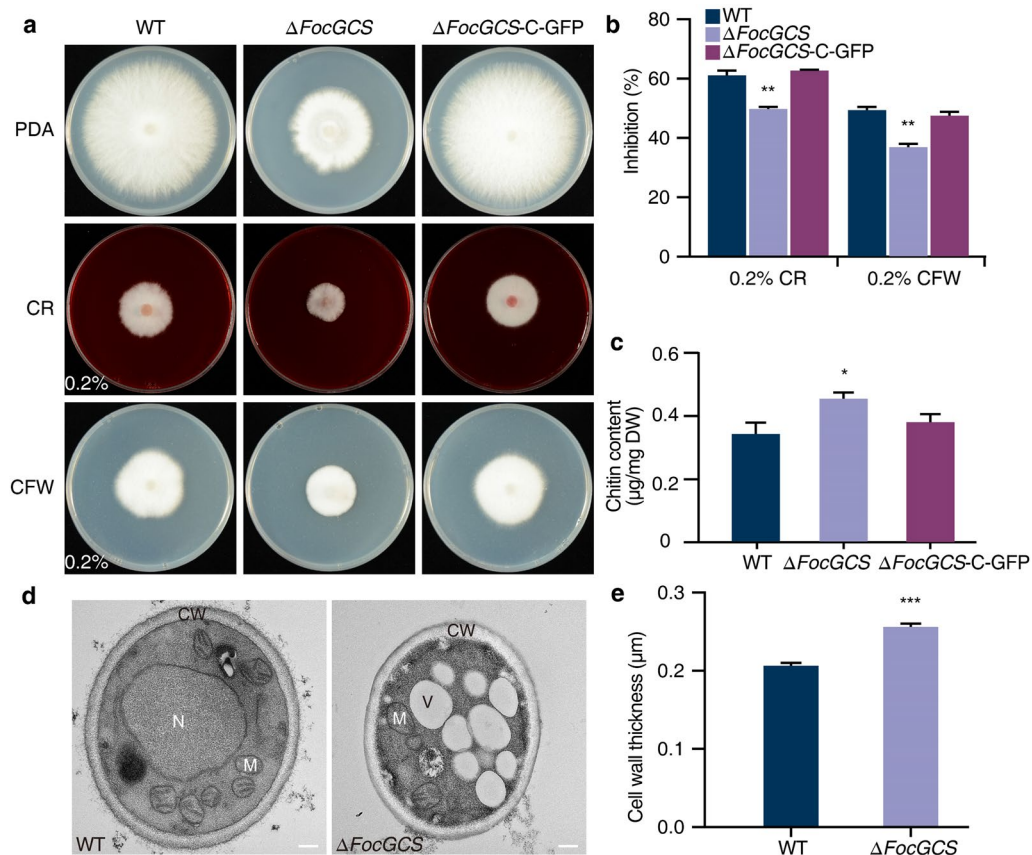


Fig. 6 Cell wall integrity analysis of the WT, $\Delta FocGCS$, and complemented strains. **a** Colony morphology of the indicated strains on PDA plates supplemented with 0.2% Calcofluor white (CFW) or 0.2% Congo red (CR). Photos were taken after incubation at 28 °C for 5 days. **b** The growth inhibition rate based on **a**. The inhibition rate was calculated by comparing the colony diameter under stress conditions with that under normal conditions. **c** Cellular chitin levels of the indicated strains measured by colorimetric determination of β -(1-4)-linked *N*-acetylglucosamine (GlcNAc). DW, dry weight. **d** Transmission electron micrographs of the WT and $\Delta FocGCS$ strains. CW, cell wall; M, mitochondrion; N, cell nucleus; V, vacuole. Scale bars = 0.2 μm . **e** Cell wall thickness of the indicated strains measured by 100 spores. The mean values \pm SD were calculated from three independent experiments, and asterisks indicate significant differences from the WT group (Student's *t*-test, * $P < 0.05$, ** $P < 0.01$, and *** $P < 0.001$)

The characterization of *FocGCS* knockout mutant in this study provides insight into the functional roles of this enzyme *in vivo*. Deletion of the putative glycosyltransferase gene in *F. graminearum*, *P. digitatum*, and *C. gloeosporioides* resulted in a complete loss of GlcCer (Ramamoorthy et al. 2007; Zhu et al. 2014; Huang et al. 2019). Our results indicate that knockout of *FocGCS* also had a dramatic effect on the synthesis of GlcCer, resulting in nearly complete GlcCer deficiency (Fig. 4a). Meanwhile, the accumulation of two direct substrates of GCS, d19:2 h18:1 and d19:2 h18:0, was substantially increased in the mutant strain (Fig. 4b). This confirmed that *FocGCS* indeed encodes a GCS that catalyzes the synthesis of GlcCer. In the $\Delta FocGCS$ mutant, inhibition of GlcCer was accompanied by severe growth defects, along with reduced production of macroconidia and formation of conidia with apparently smaller size compared with the WT strain. These results are consistent

with those reported for *A. fumigatus*, *A. nidulans*, *F. graminearum*, and *C. albicans* (Leverly et al. 2002; Ramamoorthy et al. 2007; Noble et al. 2010).

Previous reports also suggested that GlcCer affects fungal pathogenesis (Ramamoorthy et al. 2007; Huang et al. 2019). In *F. graminearum*, the growth of *FgGCS1*-knockout mutant that lacks GlcCer was retarded, but its ability in causing disease was host-dependent (Ramamoorthy et al. 2007). Pathogenicity assays indicated that the *CgGCS* deletion mutant of *C. gloeosporioides* almost completely lost the ability to invade tomato and mango hosts (Huang et al. 2019). In this study, the disease symptom in $\Delta FocGCS$ -inoculated plants was significantly reduced compared with that in WT-inoculated plants (Fig. 5), indicating that GlcCer deficiency attenuated the virulence of the pathogen. In addition, our studies showed that disruption of *FocGCS* affected cell wall integrity, which has been reported to be involved in

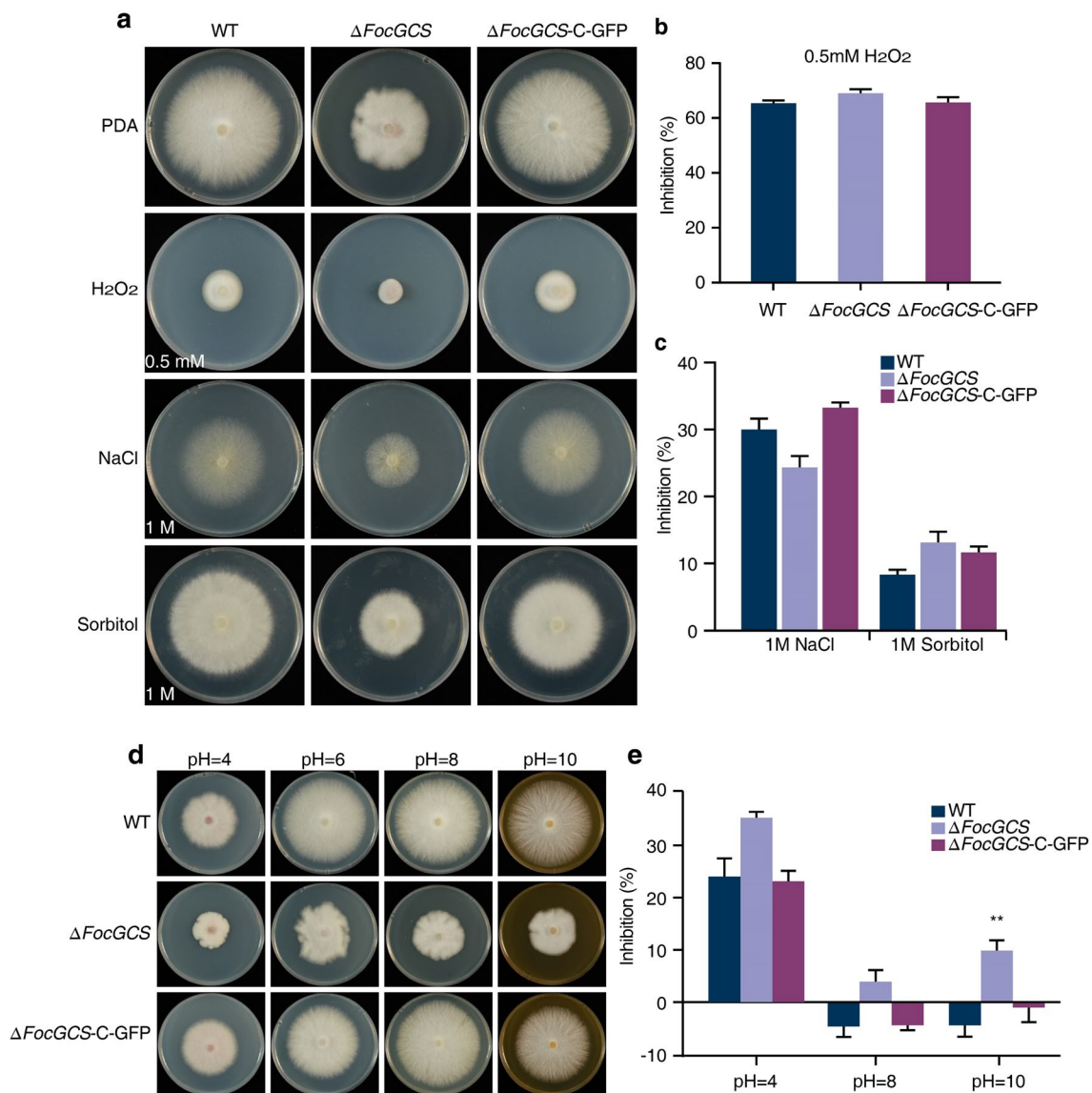
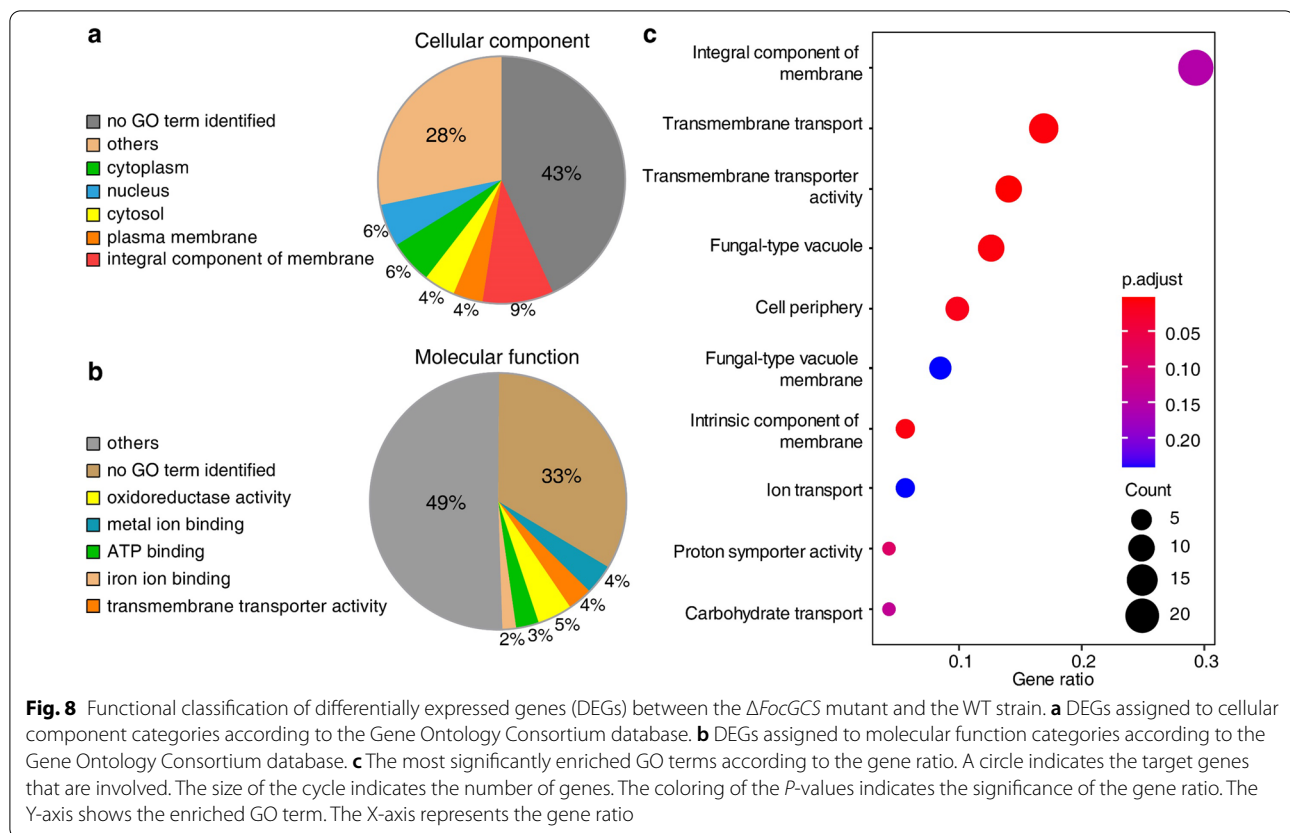


Fig. 7 Stress tolerance assays of the WT, $\Delta FocGCS$, and complemented strains. **a** Colony morphology of the indicated strains on PDA plates supplemented with 0.5 mM H₂O₂, 1 M NaCl, or 1 M sorbitol. Photos were taken after incubation at 28 °C for 5 days. **b** Colony growth inhibition incubated with 0.5 mM H₂O₂. **c** Colony growth inhibition incubated with 1 M NaCl or 1 M sorbitol. The inhibition rate was calculated by comparing the colony diameter under stress conditions with that under normal conditions. **d** Colony morphology of the indicated strains on PDA plates with different pH values. Photos were taken after incubation at 28 °C for 5 days. **e** Colony growth inhibition under different pH conditions. The inhibition rate was calculated by comparing the colony diameter under different pH conditions with that under condition of pH = 6.0. The mean values \pm SD were calculated from three independent experiments, and asterisks indicate significant differences from the WT group (Student's *t*-test, ***P* < 0.01)

virulence (Kong et al. 2012). Our transcriptome analysis showed that there was no difference in the expression of major virulence genes such as *Secreted In Xylem (SIX)*, *FocCPI1*, and *FocPGC4* genes (Additional file 3: Table S3) (Czislowski et al. 2018; Liu et al. 2019a; Dong et al. 2020). Functional classification of DEGs showed that *FocGCS* also affected transmembrane transport of *Foc TR4*, but whether transmembrane transport is related to virulence needs to be determined.

Recently, GlcCers have been reported to be involved in the regulation of pH tolerance in phytopathogens. GlcCer is critical for *C. neoformans* to grow in a neutral/alkaline but not in an acidic extracellular environment (Rittershaus et al. 2006). The *GCS* null mutant of *E. graminearum* exhibits highly reduced radial growth on solid medium, and its ability to grow at high pH is severely impaired (Ramamoorthy et al. 2007). The results of this work suggested that GlcCer in *Foc TR4* does not



broadly participate in environmental pH regulation but may have a small effect on alkali tolerance. (Fig. 7d, e). However, in the GlcCer-deficient *Foc* TR4 strain, whether the environmental pH regulation influences its pathogenesis remains to be determined.

Several studies have provided evidence that GlcCer may be important for cell wall organization in pathogenic fungi. In *C. neoformans*, GlcCer is mainly localized in the cell wall and accumulates mostly at the budding site of dividing cells (Rittershaus et al. 2006). The loss of GlcCer in *F. graminearum* results in greatly enhanced resistance to cell-wall-perturbing agents (Ramamoorthy et al. 2007; Rittenour et al. 2011). Similarly, we found that targeted disruption of *FocGCS* affects the cell wall integrity of *Foc* TR4, as the $\Delta FocGCS$ mutant displayed hyposensitivity to cell-wall-perturbing agents such as CFW and CR (Fig. 6a, b). Chitin is one of the core polysaccharide components of the fungal cell wall and is critical for maintaining infection-related morphogenesis in phytopathogenic fungi (Geoghegan et al. 2017). The deletion of chitin synthase genes in plant pathogenic fungi results in vegetative developmental defects and reduced virulence (Kong et al. 2012; Liu et al. 2016). In this study, defects in cell wall integrity in the $\Delta FocGCS$ mutant were partially

caused by the reduced chitin content (Fig. 6c). Our data provide preliminary evidence for the importance of GlcCers in cell wall organization in filamentous fungi. In addition, GCS synthesis inhibition affects membrane trafficking in *Giardia lamblia* and results in ultrastructural abnormalities including accumulation of cytosolic vesicles, enlarged lysosomes, and clathrin disorganization (Stefanic et al. 2010). As shown in Fig. 6d, we also observed the cytosolic accumulation of vesicles in the $\Delta FocGCS$ mutant. The underlying mechanism may be that GlcCer on the cytosolic side of Golgi membrane is necessary for vesicle budding.

To summarize, we characterized *FocGCS*, a gene that encodes GCS in *Foc* TR4, and provided several lines of evidence supporting the importance of *FocGCS* in regulating fungal vegetative growth, conidiation, conidial morphology, and virulence, which also corresponds with changes in the expression level of a series of functional genes in *Foc* TR4. Furthermore, *FocGCS* knockout affects cell wall integrity but not tolerance to environmental pH, osmotic, and oxidative stresses. These results establish GlcCer as a key virulence factor of *Foc* TR4, with important implications for future development of efficient management strategies for Fusarium wilt.

Conclusions

In this study, we explored the biological functions of *FocGCS* in *Foc* TR4. Loss of *FocGCS* resulted in severely retarded fungal vegetative growth, reduced conidia production, substantial loss of virulence, and abnormal conidial morphology. In addition, biochemical analyses showed that *FocGCS* affects cell wall integrity, but is not essential for tolerance to oxidative and osmotic stresses. Finally, transcriptome analysis showed that the knockout of *FocGCS* greatly influences transmembrane transport in *Foc* TR4.

Methods

Strains and growth conditions

The *Foc* TR4 strain II5 (NRRL#54,006), isolated from diseased banana in Guangdong Province of China, was used as the wild-type (WT) strain for transformation, targeted disruption, and complementation experiments in this study. The WT strain and transformants generated in this study were cultivated at 28 °C on PDA (200 g/L potato and 20 g/L dextrose, pH 7.0) medium for mycelial growth and stress tolerance assays. The mung bean liquid (MBL) (20 g mung beans boiled in water for 20 min and brought to 1 L) broth was used for conidiation assay.

Bioinformatics analysis

BLASTp was performed using human GCS protein sequence (GenBank accession no. NP_003349.1) as a query to search for homologs in the NCBI GenBank database. The protein sequences of the GCS protein family were aligned using ClustalX 2.1 and modified by GeneDoc software (Xia et al. 2006). A phylogenetic tree of putative GCS proteins identified in different organisms was constructed through the maximum likelihood (ML) method in MEGA5 software with bootstrap tests. Values on the branches of clusters represent the results of bootstrap analysis (10,000 bootstrap replicates). The Simple Modular Architecture Research Tool (SMART) was used to identify conserved protein domains of *FocGCS* (Leticnic et al. 2021).

Construction of the Δ *FocGCS* mutant and complementation strains

Targeted disruption of *FocGCS* was conducted using PEG-mediated protoplast transformation method (Yun et al. 2014). To prepare the *FocGCS* knockout construct, an 820-bp 5' flanking fragment and a 971-bp 3' flanking fragment of *FocGCS* were amplified with the primer pairs P1/P2 and P3/P4, respectively (Additional file 1: Table S2). The amplified 5' and 3' flanking sequences were fused to *HPH* driven by a constitutive *A. nidulans* *TrpC* promoter via double-joint PCR (Liu et al. 2019b).

The fusion construct was transformed into protoplasts of the WT strain II5; the Δ *FocGCS* mutant was identified through PCR assays with the primers listed in Additional file 1: Table S2 and further confirmed by Southern blot assay. Genomic DNA was isolated from the WT strain and the Δ *FocGCS* mutant using the Hi-DNA secure Plant Kit (TianGen, Beijing, China) and digested with the *Xba*I restriction enzyme. Southern blotting was performed using the DIG high prime DNA labeling and detection starter kit II (Roche, Mannheim, Germany) according to the manufacturer's protocol.

To generate the complementation strain, a *FocGCS*-*GFP* fusion cassette including the native promoter and coding sequence of *FocGCS* was inserted into plasmid pYF11, yielding the complementation vector pYF11-*FocGCS*-*GFP*. The vector was then transformed into the Δ *FocGCS* mutant; putative transformants were selected with geneticin and identified by PCR with the gene-specific primers (Additional file 1: Table S2).

Fungal growth and conidial germination assay

Mycelial growth and colony morphology of the WT and mutant strains were measured on PDA after incubation at 28 °C for 5 days. The conidia were harvested from 5-day-old PDA plates and conidial suspension was adjusted to a concentration of 1.0×10^6 conidia/mL. For the conidial germination assay, conidial suspension was added into yeast extract peptone dextrose (YEPD: 3 g/L yeast extract, 10 g/L peptone, and 20 g/L, pH 7.0) broth and incubated at 28 °C on a rotary shaker at 180 rpm for 12 h. Conidia were considered to have germinated if the length of the germination tube was more than three times that of the conidia under microscopy. The percentage of conidial germination was determined based on at least 100 randomly selected conidia for each of three replicates.

Fluorescence microscopy analysis

The Δ *FocGCS*-*C*-*GFP* strain was used for fluorescence microscopy analysis of *FocGCS* expression at different developmental stages. The nuclei of the conidia or hyphae were stained with DAPI (4',6-diamidino-2-phenylindole, Invitrogen, USA) at a final concentration of 100 nM. For fluorescence microscopic observation of conidial morphology, the conidia were stained with CFW (Calcofluor white M2R, Invitrogen, USA) according to the manufacturer's recommendations. Samples were observed under a confocal laser scanning microscope (LSM 880, Carl Zeiss, Oberkochen, Germany).

Evaluation of stress response

For cell wall sensitivity assays, 5-day-old mycelial plugs were inoculated on PDA plates supplemented with 0.2%

CFW (Phytotech, Lenexa, KS, USA) or 0.2% CR (Sigma-Aldrich, St. Louis, MO, USA). The tolerance to multiple stresses was assessed by inoculation of 5-day-old mycelial plugs on PDA containing 1 M NaCl or 1 M sorbitol for osmotic stress or 0.5 mM H₂O₂ for oxidative stress or with different pH values (4, 6, 8, and 10). After incubation at 28 °C for 5 days, the radial colony growth was measured, and growth inhibition rate was analyzed as previously described (Dai et al. 2016). The inhibition rate (%) = [(the colony diameter of control group – the colony diameter of treated group) / (the colony diameter of control group)] × 100.

Pathogenicity test and fungal biomass estimation

Cavendish banana variety Brazilian (*Musa* spp. AAA group) plantlets with 6–7 leaves and a height of 30–50 cm were used for pathogenicity test. To prepare the inoculum, 5-day-old mycelial plugs of the tested *Foc* strains were transferred into MBL broth and grown at 28 °C on a rotary shaker at 150 rpm for 5 days; the spores were collected by filtering through five layers of filter paper and the spore suspension was adjusted to a concentration of 1.0×10^7 spores/mL. The trimmed roots of the seedlings were dipped into spore suspensions for 2 min and carefully transplanted (Garcia-Bastidas et al. 2019). The disease severity was evaluated at 4 weeks after inoculation using the following rating scales: 0 = no symptom, 1 = little brown spots on the inner rhizome, 2 = less than 25% of the inner rhizome turned brown, 3 = more than 25% and less than 75% of the inner rhizome turned brown, and 4 = dead, full inner rhizome turned dark brown (Liu et al. 2019a).

Banana root samples were collected at 5, 10, and 15 dpi to estimate the fungal biomass inside the plants. The transcript levels of *FocEF1 α* and banana actin gene (*ACT1*) were determined by qPCR using gene-specific primers (Additional file 1: Table S2). The relative fungal growth *in planta* was calculated by normalizing *FocEF1 α* to banana *ACT1* and shown as ratios of *FocEF1 α* /*ACT1* (Dai et al. 2016).

HPLC–MS/MS analysis of sphingolipids

Sphingolipids were extracted as described (Bielawski et al. 2006). Conidial suspension (200 μ L, 1.0×10^6 spores/mL) from the WT, Δ *FocGCS*, or complemented strains was added into 100 mL of potato dextrose broth (PDB) and cultured for 3 days at 180 rpm. The total sphingolipids were extracted from 5 g of mycelial powder with ultrasonic extraction in 50 mL isopropanol:water:ethyl acetate (3:1:6, by vol) for 10 min. After centrifugation at 3000 *g* for 10 min, the supernatant was decanted into another tube for second round of extraction. The resultant supernatant was combined and mixed with 100 μ L of

1 mM C12 glucosylceramide (d18:1/g12:0), sphingosine (d17:1), and C12 ceramide (d18:1/c12:0) (Avanti Polar Lipids, Alabama, USA) (the internal standard for identification of GlcCers, LCBs, and Cers, respectively). C12 ceramide (d18:1/c12:0) is also the internal standard for identification of hCers. The upper organic phase containing extracted GlcCer was dried under nitrogen stream and then dissolved in 500 μ L methanol containing 0.2% formic acid and 1 mM ammonium formate.

The HPLC–MS/MS analysis was performed on an AB SCIEX 4500 triple quadrupole mass spectrometer coupled with AB SCIEX ExionLC AD LC modules (AB SCIEX, Massachusetts, USA). A 5- μ L sample was separated on a Phenomenex Luna C8 column (150 mm × 2.0 mm, 3 μ m) with a flow rate of 0.3 mL/min at 40 °C. The mobile phase solvent A was 0.2% formic acid and 2 mM ammonium formate in water. The mobile phase solvent B was 0.2% formic acid and 1 mM ammonium formate in acetonitrile. The gradient elution condition of sphingolipids was 80% B at 0–4 min, 80–90% B at 4–10 min, 90–99% B at 10–20 min, and 99% B at 20–26 min, with 80% B at 26–31 min for re-equilibration. Mass instrumentation settings and MRM settings for the targeted sphingolipid species are listed in Additional file 1: Table S4. Processing of the collected data was performed using MultiQuant software (AB SCIEX).

Measurement of chitin content

Chitin content was measured according to a previously described method (Bulik et al. 2003; Dai et al. 2016). The cellular chitin levels were measured using colorimetric determination of β -(1–4)-linked *N*-acetylglucosamine (GlcNAc). Briefly, 10 mg of ground mycelial powder, from strains cultured in YEPD liquid medium for 3 days, was suspended in 1 mL of 6% KOH and heated at 80 °C for 90 min. After centrifugation at 12,000 *g* for 10 min, the pellets were suspended in 1 mL phosphate-buffered saline (PBS, pH 7.4) and spun again, and the buffer was discarded. Then, each pellet was suspended in 0.1 mL of McIlvaine buffer (pH 6.0) containing 5 μ L chitinase from *Streptomyces griseus* (5 mg/mL in PBS) and incubated at 37 °C for 24 h. Ten microliters of sample supernatant and 10 μ L 0.27 M sodium borate (pH 9.0) were combined and heated for 10 min at 100 °C. After immediately cooling to room temperature, 100 μ L of the freshly diluted DMAB solution (10 g of *p*-dimethylaminobenzaldehyde in 12.5 mL of concentrated HCl and 87.5 mL of glacial acetic acid, diluted 1:10 with glacial acetic acid) was added to the samples and incubated at 37 °C for 20 min. The quantity of glucosamine in samples was calculated by a standard curve prepared with GlcNAc by recording the absorbance at 585 nm.

Transmission electron microscopy

For TEM observation, conidia were collected from 5-day-old PDA plates. Samples were fixed in 2.5% (v/v) glutaraldehyde and 2% (v/v) paraformaldehyde in 0.1 M phosphate-buffered saline (pH 7.4). After being washed with the buffer, specimens were post-fixed for 21 h with 1% potassium permanganate at 4 °C. Samples were embedded in SPI-PON812 resin (SPI Supplies). Ultrathin sections were obtained on a microtome (Leica EM UC6) and stained with 2% uranyl acetate followed by 3% lead citrate. The images were photographed using a transmission electron microscope (JEM-1400Flash) at an accelerating voltage of 120 kV.

Gene expression analysis

Total RNA was isolated from 100 mg of frozen hyphae or banana roots using a Plant RNA Kit (Omega, Georgia, USA). The first-strand cDNA was synthesized from 1 µg total RNA using the PrimeScript 1st Strand cDNA Synthesis Kit (TAKARA, Dalian, China) according to the manufacturer's instructions, and the samples were diluted 1:5 with RNase-free distilled water. qPCR was performed with three technical replicates using the Applied Biosystems StepOnePlus System as described previously (Huang et al. 2019). The *FocEF1α* gene was used as an internal control to normalize the data for comparing the relative transcript abundance. The relative expression of each gene under different conditions was determined using the $2^{-\Delta\Delta CT}$ method (Livak and Schmittgen 2001). All the primer pairs are listed in Additional file 1: Table S2.

Transcriptome analysis

Conidia (1.0×10^6 conidia/mL) of the WT and $\Delta FocGCS$ strains were cultured in PDB for 3 days at 180 rpm. The hyphae were collected by filtering through five layers of filter paper, washed three times with sterile distilled water, and vigorously ground into a fine powder using liquid nitrogen (Huang et al. 2019). Total RNA was isolated from frozen hyphae powder using the Plant RNA Kit (Omega, Georgia, USA). RNA purity was checked using the NanoDrop spectrophotometer (IMPLEN, CA, USA). The library preparations were sequenced on an Illumina HiSeq 2000 platform.

Statistical analysis

All experiments were repeated independently three times, and each experiment was set with three technical replicates. Data were analyzed using Student's unpaired *t*-tests in SPSS (SPSS, Chicago, USA).

Abbreviations

Cers: Ceramides; CFW: Calcofluor white; CR: Congo red; DEGs: Differentially expressed genes; dpi: Days post-inoculation; *Foc*: *Fusarium oxysporum* f. sp. *cubense*; *Foc* TR4: *Fusarium oxysporum* f. sp. *cubense* tropical race 4; GCS: Glucosylceramide synthase; GFP: Green fluorescent protein; GlcCers: Glucosylceramides; GlcNAC: *N*-Acetylglucosamine; GO: Gene Ontology; hCers: Hydroxyceramides; HPH: Hygromycin-B 4-O-kinase; HPLC-MS/MS: High-performance liquid chromatography-mass spectrometry/mass spectrometry; LCBS: Long chain bases; MBL: Mung bean liquid; PBS: Phosphate-buffered saline; PDA: Potato dextrose agar; PDMP: 1-Phenyl-2-decanoylamino-3-morpholino-1-propanol; *SIX*: *Secreted In Xylem*; TEM: Transmission electron microscopy; WT: Wild type; YEPD: Yeast extract peptone dextrose.

Supplementary information

The online version contains supplementary material available at <https://doi.org/10.1186/s42483-022-00136-y>.

Additional file 1: Table S1. Sequence identity of *FocGCS* with *GCS* from other organisms. **Table S2.** PCR primers used in this study. **Table S4.** Mass spectrometer parameters used for MRM scanning of sphingolipid species.

Additional file 2: Figure S1. Domain organization of *FocGCS* and multiple sequence alignment of GCSs from different organisms. **Figure S2.** Green fluorescence from *FocGCS*-GFP was observed in conidia and hyphae of the $\Delta FocGCS$ -C-GFP strain. **Figure S3.** Characterization of *FocGCS*-knockout strain ($\Delta FocGCS$) and complementation strain ($\Delta FocGCS$ -C-GFP). **Figure S4.** HPLC-MS/MS chromatograms showing the structure and retention time of main hydroxyceramides in *Foc* TR4 and $\Delta FocGCS$ strains.

Additional file 3: Table S3. Detailed information of differentially expressed genes.

Acknowledgements

Not applicable.

Authors' contributions

JW and NY conceived and designed the project, jointly performed data analysis and wrote the manuscript. JW conducted most of the experiments. KZ, NH, HNB, and LQH contributed part of experiments and analyzed data. YBY, SWL, and CYL contributed reagents/material tools. All authors read and approved the final manuscript.

Funding

This work was supported by the funds from the National Natural Science Foundation of China (32070196), the Natural Science Foundation of Guangdong Province (2019B1515120088), and Department of Science and Technology of Guangdong Province (33000-42021182), and by the Fundamental Research Funds for the Central Universities, Sun Yat-sen University (33000-31611238).

Availability of data and materials

The datasets used and/or analyzed during the current study are available from the corresponding author on reasonable request.

Declarations

Ethics approval and consent to participate

Not applicable.

Consent for publication

Not applicable.

Competing interests

The authors declare that they have no competing interests.

Author details

¹State Key Laboratory of Biocontrol and Guangdong Provincial Key Laboratory of Plant Resource, Sun Yat-sen University, Guangzhou 510275, China. ²School of Life Sciences, Sun Yat-sen University, Guangzhou 510275, China. ³School

of Agriculture, Sun Yat-sen University, Shenzhen 518107, China. ⁴Key Laboratory of South Subtropical Fruit Biology and Genetic Resource Utilization, Ministry of Agriculture, Key Laboratory of Tropical and Subtropical Fruit Tree Research of Guangdong Province, Institute of Fruit Tree Research, Guangdong Academy of Agricultural Sciences, Guangzhou 510640, China.

Received: 7 April 2022 Accepted: 9 August 2022

Published online: 18 August 2022

References

- Bielawski J, Szulc ZM, Hannun YA, Bielawska A. Simultaneous quantitative analysis of bioactive sphingolipids by high-performance liquid chromatography-tandem mass spectrometry. *Methods*. 2006;39:82–91. <https://doi.org/10.1016/j.ymeth.2006.05.004>.
- Bulik DA, Olczak M, Lucero HA, Osmond BC, Robbins PW, Specht CA. Chitin synthesis in *Saccharomyces cerevisiae* in response to supplementation of growth medium with glucosamine and cell wall stress. *Eukaryot Cell*. 2003;2:886–900. <https://doi.org/10.1128/EC.2.5.886-900.2003>.
- Czislowski E, Fraser-Smith S, Zander M, O'Neill WT, Meldrum RA, Tran-Nguyen L, et al. Investigation of the diversity of effector genes in the banana pathogen, *Fusarium oxysporum* f. sp. *cubense*, reveals evidence of horizontal gene transfer. *Mol Plant Pathol*. 2018;19(5):1155–71. <https://doi.org/10.1111/mpp.12594>.
- Dai Y, Cao ZY, Huang LH, Liu SX, Shen ZH, Wang YY, et al. CCR4-Not complex subunit Not2 plays critical roles in vegetative growth, conidiation and virulence in watermelon fusarium wilt pathogen *Fusarium oxysporum* f. sp. *niveum*. *Front Microbiol*. 2016. <https://doi.org/10.3389/fmicb.2016.01449>.
- Del Poeta M, Nimrichter L, Rodrigues ML, Luberto C. Synthesis and biological properties of fungal glucosylceramide. *PLoS Pathog*. 2014. <https://doi.org/10.1371/journal.ppat.1003832>.
- Dickson RC, Lester RL. Sphingolipid functions in *Saccharomyces cerevisiae*. *Biochim Biophys Acta*. 2002;1583(1):13–25. [https://doi.org/10.1016/S1388-1981\(02\)00210-X](https://doi.org/10.1016/S1388-1981(02)00210-X).
- Dita MA, Waalwijk C, Buddenhagen IW, Souza MT, Kema GHJ. A molecular diagnostic for tropical race 4 of the banana fusarium wilt pathogen. *Plant Pathol*. 2010;59:348–57. <https://doi.org/10.1111/j.1365-3059.2009.02221.x>.
- Dong ZY, Luo M, Wang ZZ. An exo-polygalacturonase Pgc4 regulates aerial hyphal growth and virulence in *Fusarium oxysporum* f. sp. *cubense* race 4. *Int J Mol Sci*. 2020;21(16):5886. <https://doi.org/10.3390/ijms21165886>.
- Fernandes CM, de Castro PA, Singh A, Fonseca FL, Pereira MD, Vila TVM, et al. Functional characterization of the *Aspergillus nidulans* glucosylceramide pathway reveals that LCB Delta 8-desaturation and C9-methylation are relevant to filamentous growth, lipid raft localization and Psd1 defensin activity. *Mol Microbiol*. 2016;102:488–505. <https://doi.org/10.1111/mmi.13474>.
- Fourie G, Steenkamp ET, Gordon TR, Viljoen A. Evolutionary relationships among the *Fusarium oxysporum* f. sp. *cubense* vegetative compatibility groups. *Appl Environ Microb*. 2009;75:4770–81. <https://doi.org/10.1128/AEM.00370-09>.
- Garcia-Bastidas FA, van der Veen AJT, Nakasato-Tagami G, Meijer HJG, Arango-Isaza RE, Kema GHJ. An improved phenotyping protocol for Panama disease in banana. *Front Plant Sci*. 2019. <https://doi.org/10.3389/fpls.2019.01006>.
- Geoghegan I, Steinberg G, Gurr S. The role of the fungal cell wall in the infection of plants. *Trends Microbiol*. 2017;25:957–67. <https://doi.org/10.1016/j.tim.2017.05.015>.
- Huang YM, Li B, Yin J, Yang QS, Sheng O, Deng GM, et al. CgGCS, encoding a glucosylceramide synthase, is required for growth, conidiation and pathogenicity in *Colletotrichum gloeosporioides*. *Front Microbiol*. 2019. <https://doi.org/10.3389/fmicb.2019.01016>.
- Kong LA, Yang J, Li GT, Qi LL, Zhang YJ, Wang CF, et al. Different chitin synthase genes are required for various developmental and plant infection processes in the rice blast fungus *Magnaporthe oryzae*. *PLoS Pathog*. 2012. <https://doi.org/10.1371/journal.ppat.1002526>.
- Leipelt M, Warnecke D, Zähringer U, Ott C, Müller F, Hube B, et al. Glucosylceramide synthases, a gene family responsible for the biosynthesis of glucosylsphingolipids in animals, plants, and fungi. *J Biol Chem*. 2001;276:33621–9. <https://doi.org/10.1074/jbc.M104952200>.
- Leticia I, Khedkar S, Bork P. SMART: recent updates, new developments and status in 2020. *Nucleic Acids Res*. 2021;49:D458–60. <https://doi.org/10.1093/nar/gkaa937>.
- Leverly SB, Momany M, Lindsey R, Toledo MS, Shayman JA, Fuller M, et al. Disruption of the glucosylceramide biosynthetic pathway in *Aspergillus nidulans* and *Aspergillus fumigatus* by inhibitors of UDP-Glc:ceramide glucosyltransferase strongly affects spore germination, cell cycle, and hyphal growth. *FEBS Lett*. 2002;525:59–64. [https://doi.org/10.1016/S0014-5793\(02\)03067-3](https://doi.org/10.1016/S0014-5793(02)03067-3).
- Li CY, Chen S, Zuo CW, Sun QM, Ye Q, Yi GJ, et al. The use of GFP-transformed isolates to study infection of banana with *Fusarium oxysporum* f. sp. *cubense* race 4. *Eur J Plant Pathol*. 2011;131:327–40. <https://doi.org/10.1007/s10658-011-9811-5>.
- Liu ZY, Zhang XP, Liu X, Fu CY, Han XY, Yin YN, et al. The chitin synthase FgChs2 and other FgChss co-regulate vegetative development and virulence in *F. graminearum*. *Sci Rep*. 2016. <https://doi.org/10.1038/srep34975>.
- Liu SW, Wu B, Yang J, Bi FC, Dong T, Yang QS, et al. A cerato-platanin family protein FocCP1 is essential for the penetration and virulence of *Fusarium oxysporum* f. sp. *cubense* tropical race 4. *Int J Mol Sci*. 2019a. <https://doi.org/10.3390/ijms20153785>.
- Liu ZY, Jian YQ, Chen Y, Kistler HC, He P, Ma ZH, et al. A phosphorylated transcription factor regulates sterol biosynthesis in *Fusarium graminearum*. *Nat Commun*. 2019b. <https://doi.org/10.1038/s41467-019-09145-6>.
- Livak KJ, Schmittgen TD. Analysis of relative gene expression data using real-time quantitative PCR and the 2^(-T)(-Delta Delta C) method. *Methods*. 2001;25:402–8. <https://doi.org/10.1006/meth.2001.1262>.
- Molina AB, Fabregar E, Sinohin VG, Yi G, Viljoen A. Recent occurrence of *Fusarium oxysporum* f. sp. *cubense* tropical race 4 in Asia. *Acta Hort*. 2009;828:109–15. <https://doi.org/10.17660/ActaHortic.2009.828.10>.
- Nimrichter L, Rodrigues ML. Fungal glucosylceramides: from structural components to biologically active targets of new antimicrobials. *Front Microbiol*. 2011. <https://doi.org/10.3389/fmicb.2011.00212>.
- Noble SM, French S, Kohn LA, Chen V, Johnson AD. Systematic screens of a *Candida albicans* homozygous deletion library decouple morphogenetic switching and pathogenicity. *Nat Genet*. 2010;42:590–8. <https://doi.org/10.1038/ng.605>.
- Ploetz RC. *Fusarium*-induced diseases of tropical, perennial crops. *Phytopathology*. 2006;96:648–52. <https://doi.org/10.1094/PHYTO-96-0648>.
- Ploetz RC. Management of *Fusarium* wilt of banana: a review with special reference to tropical race 4. *Crop Prot*. 2015;73:7–15. <https://doi.org/10.1016/j.cpro.2015.01.007>.
- Qi XZ, Guo LJ, Yang LY, Huang JS. Foatf1, a bZIP transcription factor of *Fusarium oxysporum* f. sp. *cubense*, is involved in pathogenesis by regulating the oxidative stress responses of Cavendish banana (*Musa* spp.). *Physiol Mol Plant Pathol*. 2013;84:76–85. <https://doi.org/10.1016/j.pmp.2013.07.007>.
- Ramamoorthy V, Cahoon EB, Li J, Thokala M, Minto RE, Shah DM. Glucosylceramide synthase is essential for alfalfa defensin-mediated growth inhibition but not for pathogenicity of *Fusarium graminearum*. *Mol Microbiol*. 2007;66:771–86. <https://doi.org/10.1111/j.1365-2958.2007.05955.x>.
- Rittenour WR, Chen M, Cahoon EB, Harris SD. Control of glucosylceramide production and morphogenesis by the Bar1 ceramide synthase in *Fusarium graminearum*. *PLoS ONE*. 2011;6: e19385. <https://doi.org/10.1371/journal.pone.0019385>.
- Rittershaus PC, Kechichian TB, Allegood JC, Merrill AH, Hennig M, Luberto C, et al. Glucosylceramide synthase is an essential regulator of pathogenicity of *Cryptococcus neoformans*. *J Clin Invest*. 2006;116:1651–9. <https://doi.org/10.1172/JCI27890>.
- Rodrigues ML, Travassos LR, Miranda KR, Franzen AJ, Rozental S, de Souza W, et al. Human antibodies against a purified glucosylceramide from *Cryptococcus neoformans* inhibit cell budding and fungal growth. *Infect Immun*. 2000;68:7049–60. <https://doi.org/10.1128/IAI.68.12.7049-7060.2000>.
- Schoffelmeer EAM, Klis FM, Sietsma JH, Cornelissen BJC. The cell wall of *Fusarium oxysporum*. *Fungal Genet Biol*. 1999;27:275–82. <https://doi.org/10.1006/fgbi.1999.1153>.
- Stefanic S, Spycher C, Morf L, Fabrias G, Casas J, Schraner E, et al. Glucosylceramide synthesis inhibition affects cell cycle progression, membrane trafficking, and stage differentiation in *Giardia lamblia*. *J Lipid Res*. 2010;51:2527–45. <https://doi.org/10.1194/jlr.M003392>.
- Thevisen K, Warnecke DC, Francois IE, Leipelt M, Heinz E, Ott C, et al. Defensins from insects and plants interact with fungal glucosylceramides. *J Biol Chem*. 2004;279:3900–5. <https://doi.org/10.1074/jbc.M311165200>.

- Wang J, Chen YL, Li YK, Chen DK, He JF, Yao N. Functions of sphingolipids in pathogenesis during host-pathogen interactions. *Front Microbiol.* 2021;12: 701041. <https://doi.org/10.3389/fmicb.2021.701041>.
- Warnecke D, Heinz E. Recently discovered functions of glucosylceramides in plants and fungi. *Cell Mol Life Sci.* 2003;60:919–41. <https://doi.org/10.1007/s00018-003-2243-4>.
- Xia AH, Zhou QX, Yu LL, Li WG, Yi YZ, Zhang YZ, et al. Identification and analysis of YELLOW protein family genes in the silkworm, *Bombyx mori*. *BMC Genomics.* 2006. <https://doi.org/10.1186/1471-2164-7-195>.
- Yun YZ, Liu ZY, Zhang JZ, Shim WB, Chen Y, Ma ZH. The MAPKK FgMkk1 of *Fusarium graminearum* regulates vegetative differentiation, multiple stress response, and virulence via the cell wall integrity and high-osmolarity glycerol signaling pathways. *Environ Microbiol.* 2014;16:2023–37. <https://doi.org/10.1111/1462-2920.12334>.
- Zhu C, Wang M, Wang W, Ruan R, Ma H, Mao C, et al. Glucosylceramides are required for mycelial growth and full virulence in *Penicillium digitatum*. *Biochem Biophys Res Commun.* 2014;455:165–71. <https://doi.org/10.1016/j.bbrc.2014.10.142>.
- Zuo CW, Li CY, Li B, Wei YR, Hu CH, Yang QS, et al. The toxic mechanism and bioactive components of Chinese leek root exudates acting against *Fusarium oxysporum* f. sp. *cubense* tropical race 4. *Eur J Plant Pathol.* 2015;143:447–60. <https://doi.org/10.1007/s10658-015-0697-5>.

Ready to submit your research? Choose BMC and benefit from:

- fast, convenient online submission
- thorough peer review by experienced researchers in your field
- rapid publication on acceptance
- support for research data, including large and complex data types
- gold Open Access which fosters wider collaboration and increased citations
- maximum visibility for your research: over 100M website views per year

At BMC, research is always in progress.

Learn more biomedcentral.com/submissions

